

# Numerical Assessment of Factor B in Mathews' Method for Open Stope Design

R.P. Bewick, P.Eng., M.A.Sc.  
*Golder Associates Ltd., Sudbury, ON, Canada*

P.K. Kaiser, P.Eng., Ph.D.  
*Center for Excellence in Mining Innovation (CEMI), Sudbury, ON, Canada*

**ABSTRACT:** A numerical modelling study was completed to derive the Factor B curves proposed by Mathews et al. (1980) & Potvin et al. (1988) to further understand the relationship between joint orientation and stope stability. A continuum finite element modelling approach which included joint elements was adopted to back-analyse and assess the influence of various joint properties and stress states on the shape of the Factor B curve. This paper provides insight into mechanisms affecting the shape of the Factor B curve. A better understanding of factors controlling the *B*-value potentially reduces some of the conservatism in the design of open stopes and other underground excavations.

## 1 INTRODUCTION

The stability graph method developed by Mathews et al. (1980), later modified by Potvin et al. (1988), Clark (1998), Suorineni (1999a, 1999b, 2000), and Capes et al. (2005) amongst others, is an empirical approach that has been developed for open stope design based on the depth of mining, rock mass quality and stope span. The stability graph is a plot of stope hydraulic radius versus the modified stability number,  $N'$ , which is defined as:

$$N' = Q' \cdot A \cdot B \cdot C \quad (1)$$

where  $Q'$  = the modified Q rock mass classification (Barton et al., 1974);  $A$  = the rock stress factor;  $B$  = the joint orientation adjustment factor – Factor B; and  $C$  = the gravity adjustment factor.

The Factor B is used to account for the influence of the relative orientation of dominate jointing relative to the excavation surface (stope wall or back) being assessed. The relative angle is referred to as the angle  $\beta$ . It was included as a modifying factor in  $N'$  because the influence of joint orientation relative to an excavation surface is not considered in the Q classification system (Suorineni, 1999a).

The original Factor B proposed by Mathews et al. (1980) was based on expert discussion which considered change of behaviour based on the direction of loading with respect to the inclination of a plane of weakness (Figure 1). The revised Factor B curve which was based on a larger number of case histories after Potvin et al. (1988) is presented on Figure 2. The assumptions behind each of the curve's respective shape are also presented in these figures.

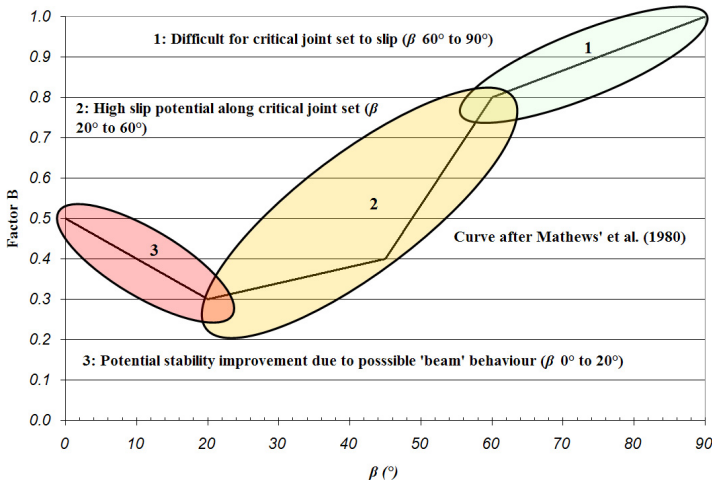


Figure 1: Factor B curve after Mathews et al. (1980) and underlying assumptions regarding its shape.

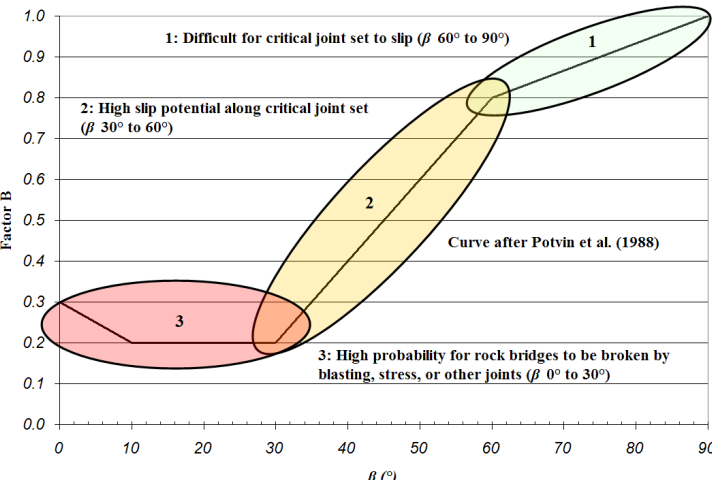


Figure 2: Factor B curve after Potvin et al. (1988) and underlying assumptions regarding its shape.

The main difference between the curves proposed by Mathews et al. and Potvin et al. is between  $\beta$  angles of 0° and 45°. Mathews et al. (1980) assumed that there was a potential stability improvement as the dominant joint set becomes parallel to the excavation boundary as a result of potential ‘beam’ behaviour. Potvin et al. (1988) observed that most structurally controlled failures occurred along joints having a shallow angle (0° to 30°) with respect to the exposed excavation boundaries. The interpretation by Potvin et al. was that the smaller the difference in the dip of the major critical joint set and the excavation boundary, the greater the probability of having rock bridges fail and joints separate by blasting, stress/relaxation, or by other intersecting joint sets.

Both the Factor B curves of Mathews et al. and Potvin et al. were scaled assuming that joints oriented at an angle of 90° to the slope boundary had no to little effect on stability as failure is difficult to mobilize ( $B = 1.0$ ). Potvin et al. suggested an adjustment of 0.2 for a small critical joint angle (i.e.  $\beta$  angles of 10° to 30° to the slope boundary) and stated that the best results were obtained by setting an orientation adjustment of 0.3 for the common case of a joint dipping sub-parallel to the slope face ( $\beta$  angles of 0° to 10° to the slope boundary).

In addition to the general Factor B, Potvin (1988) proposed a Factor B chart for vertical joints and near vertical slope faces which takes into account the difference in strike between the joint and the slope face. Potvin et al. also mention the influence of joint friction as a potential stability enhancer and assumed that joint friction was taken into account within  $N'$  through the  $Q'$  parameter's  $J_r/J_a$  ratio.

## 2 MODELLING THE FACTOR B

### 2.1 The Model, Geometry & Input Parameters

The program Phase<sup>2</sup> (©RocScience, 2006) was used for the modelling and to assess the influence of various joint properties and states of stress on the shape of the Factor B curve. The purpose was to determine if a 2D continuum finite element modelling approach could account for discrete structures through the use of joint elements.

An open unsupported slope of typical size for Canadian hard rock mines (based on the Authors experience with mines located in the Canadian Shield and Sudbury Ontario Basin) was modelled: 30m x 10m (height x span) dipping 80°. This slope geometry was also comparable to the “average” sublevel slope geometry determined by Zhang & Mitri (2007).

Models were created based on the joint orientations ( $\beta$ ) of 90°, 60°, 45°, 20°, and 0° to the slope hanging wall and back.

The rock mass was considered isotropic with plastic behaviour. The Mohr-Coulomb failure criterion was used with a tension cut off. The strength parameters of the rock mass are listed in Table 1 and were chosen to represent typical hard rock modelling parameters.

The following two assumptions were used to assist in the selection of the joint strength parameters: (1) influence of rock bridging could be taken into account by increasing the cohesion of the joints; and (2) joint properties were to be chosen such that no joint yield could occur under in situ stress conditions. The strength parameters for the joints are listed in Table 1. For this study the baseline joint normal stiffness was assumed to be one order of magnitude higher than the modulus of the rock mass and the baseline joint shear stiffness was assumed to be equal to the modulus of the rock mass. These values were used because they typically ensure model solution convergence and provide reasonable modelling results for joints which behave in a brittle manner (Corkum, 2007, Bewick, 2008). The joint cohesion was set to 0.75 MPa to account for the strength increase from rock bridges along the modelled fully persistent joints.

The state of stress used in the models is representative for a depth of 1000 m and the vertical stress component was set for a  $\gamma = 0.027 \text{ MN/m}^3$ .

Table 1. Model Baseline Parameters

Rock Mass		Joint Elements	
Parameter	Value	Parameter	Value
$\sigma_c$	150 MPa	$\phi$	40°
$m_i$	20	$c$	0.75 MPa
$E_m$	30 GPa	$\sigma_t$	$1e^{-5}$ MPa
$\phi$	52°	$K_n$	300 GPa
$\phi_r$	26°	$K_s$	30 GPa
$c$	15 MPa	$K_n/K_s$	10
$c_r$	7.5 MPa		
$\nu$	0.25		

### 2.2 Back-Analysis Procedure

Cai et al. (1999) analysed 26 large scale underground excavations of comparable size to the chosen slope dimensions, to assess civil support design practice. Through back-analyses using 2D finite element modelling of the case histories, Cai et al. determined that the typical support element length chosen for supporting the sidewalls of the assessed 26 large underground caverns corresponded approximately to the maximum depth of the  $\sigma_3 = 0.5 \text{ MPa}$  contour limit (Figure 3). For civil engineering projects, it is assumed that support elements must be long enough to anchor into sound (elastic) ground and reduce the loosening of the rock mass. The zone defined by the  $\sigma_3 = 0.5 \text{ MPa}$  contour line can be assumed to be representative of the loosening zone.

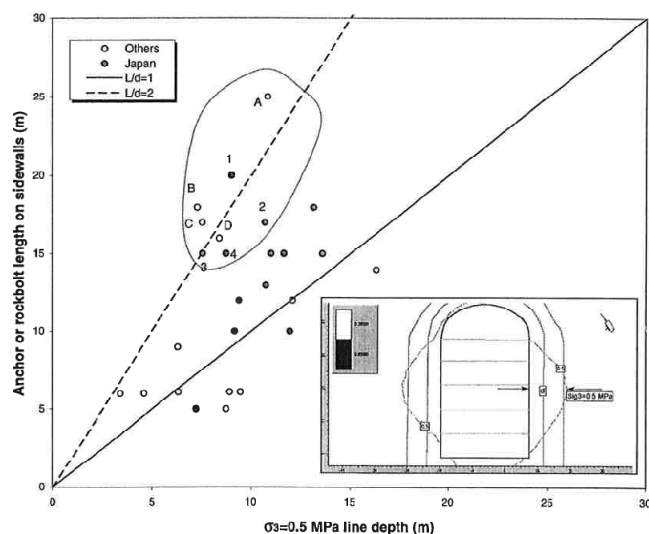


Figure 3: Results from Cai et al. (1999) showing the general trend of sidewall support length equal to the  $\sigma_3 = 0.5$  MPa contour limit. There is a cluster of data points (encircled) which represent support lengths around 2 times that of the 0.5 MPa limit. According to Cai et al., no clear reason could be identified for the use of the large reinforcement lengths at those sites.

Cai et al.'s selected confinement ( $\sigma_3 = 0.5$  MPa) criterion is similar to that discussed by Alcott & Kaiser (1999) where they grouped slope stability by three confinement levels:

- $\sigma_3 = 0$  MPa contour: a zone where there is loss of confinement and the potential for failure along major structure (faults, contacts, shear zones, etc.);
- $\sigma_3 = -5$  MPa contour: a zone where the tensile strength of the rock mass is exceeded (for rock masses with RMR ranging 75 to 85) and there is potential for failure of rock masses with critically orientated minor structure (persistent joints); and
- $\sigma_3 = -10$  MPa contour: a zone where the tensile strength of the intact rock is exceeded and there is failure potential regardless of structure.

Based on the above studies, a confinement based minor principal stress ( $\sigma_3$ ) criteria was chosen to assess the influence of joint orientation on open slope stability and to numerically derive the Factor B curves. The  $\sigma_3 = 0.5$  MPa limit was selected because it is assumed that this zone represents the area of potential rock mass loosening as discussed by Cai et al. (1999).

### 2.2.1 Derivation of the Factor B Curve from Models

The maximum depth of the  $\sigma_3 = 0.5$  MPa contour limit was measured perpendicular to the hanging wall and stope back for each of the  $\beta$  angle cases analysed to recreate the Factor B curve. The results for the footwall are not discussed here because the footwall geometry is nearly identical to the hanging wall geometry which produces almost identical results. Furthermore, the sidewalls are not discussed because the modelling only considers the 2D plain strain case which does not allow for the sidewalls of the stopes to be modelled. It is understood that 3-dimensional effects may influence results where structures are free to move on both connected excavation faces.

The measurements of the chosen confinement limit in the models were then normalized by dividing by the depth of  $\sigma_3 = 0.5$  MPa contour limit for the same stope geometry with the same material properties but containing joints oriented  $90^\circ$  to the stope wall. This process can be summarized by the following equation:

$$\text{Numerical Factor } B = \left( \frac{d_{\sigma_3\beta}}{d_{\sigma_3\beta=90}} \right)^{-1} \quad (2)$$

where  $d_{\sigma_3\beta}$  is the depth of  $\sigma_3 = 0.5$  MPa contour limit for different  $\beta$  angles and  $d_{\sigma_3\beta=90}$  is the depth of  $\sigma_3 = 0.5$  MPa contour limit for the baseline finite element model where the joints are orientated  $90^\circ$  to the slope face being assessed. The results are normalized in this manner because joints oriented  $90^\circ$  to the slope face are assumed to have little to no influence on stability (Mathews et al., 1980 & Potvin et al., 1988).

### 3 POTENTIAL MECHANISMS CONTROLLING THE FACTOR B CURVE

#### 3.1 Hanging Wall

A set of numerically derived Factor B results for the slope hanging wall are presented on Figure 4 and can be divided into two sections; (1) between  $0^\circ$  and  $<45^\circ$  where the numerical curve does not match the empirically derived curves; and (2) between  $45^\circ$  and  $90^\circ$  where the numerical curve fits well to the empirically derived curves based on the assessment of confinement change around the slope hanging wall boundary alone.

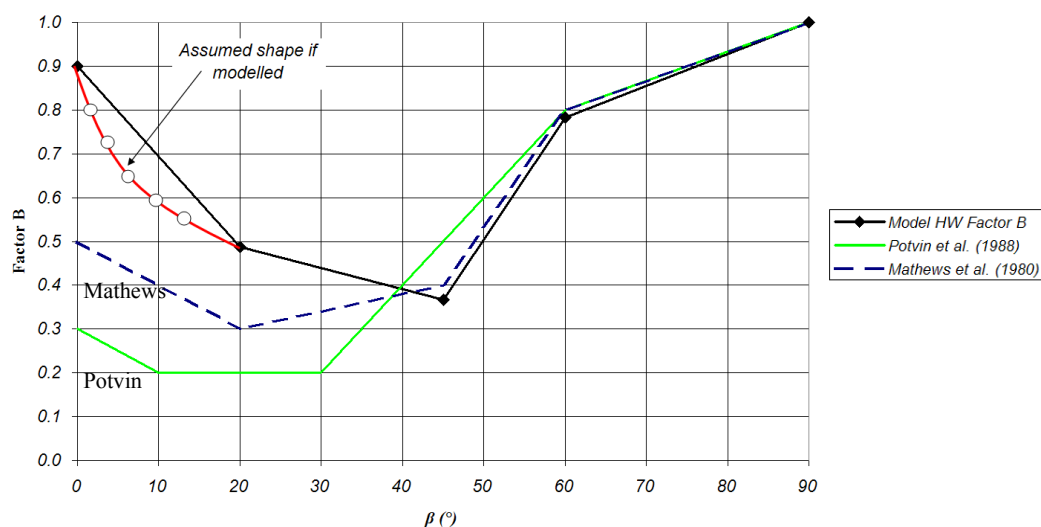


Figure 4: Example set of modelling results for joint spacing = 2m,  $K_n/K_s = 10$ ,  $k_o = 1$ , and  $\phi = 40^\circ$ .

Looking specifically at the results for joints parallel ( $\beta = 0^\circ$ ) to the slope hanging wall with a joint spacing of 2 m (Figure 5), it is observed that this orientation of jointing has little influence on changing confinement around the slope boundary. This is only observed for the case of a  $\beta$  angle of  $0^\circ$  and thick bedding (modelled 2 m joint spacing) but not for  $\beta$  angles of  $20^\circ$ ,  $45^\circ$ ,  $60^\circ$ , and  $90^\circ$  which significantly influence the state of confinement around the slope boundary as shown on Figure 6. This suggests that low joint confinement is dominating or controlling the shape of the  $B$ -curve at relative joint angles  $>45^\circ$ .

The results illustrated on Figure 6 (see numbers on Figure 6) also suggest that; (1) the shear yield, (x) pattern predicted by the models, appears to be controlled by the orientation and location of the joints in the slope back (i.e. joint slip appears to constrain the extent of predicted rock mass yield); and (2) there is higher dilution potential with joints oriented  $45^\circ$  and  $60^\circ$  to the slope boundary as confinement is pushed even deeper away due to the orientation of the joint elements. Thus, it is expected that a more rapid drop in  $B$  would occur than shown by the current linear connection of modelling points (see curved line and hollow dots on Figure 4).

Potvin et al. (1988) proposed through the examination of case history data that stability was controlled by the breakage of rock bridges due to blasting, stress, other rock joints, etc., when joints are oriented at shallow angles with respect to the slope face (i.e.  $\beta$  approximately between  $10^\circ$  and  $<45^\circ$ ) suggesting a different control on stability at these relative shallow joint angles.

The instability resulting from the degradation described by Potvin et al. (1988) could also be argued as stability being controlled by degraded inter-joint rock mass strength around the slope

boundary. Where inter-joint rock mass strength refers to the strength of the rock mass between the modelled joint elements (i.e. rock material bound by the joints).

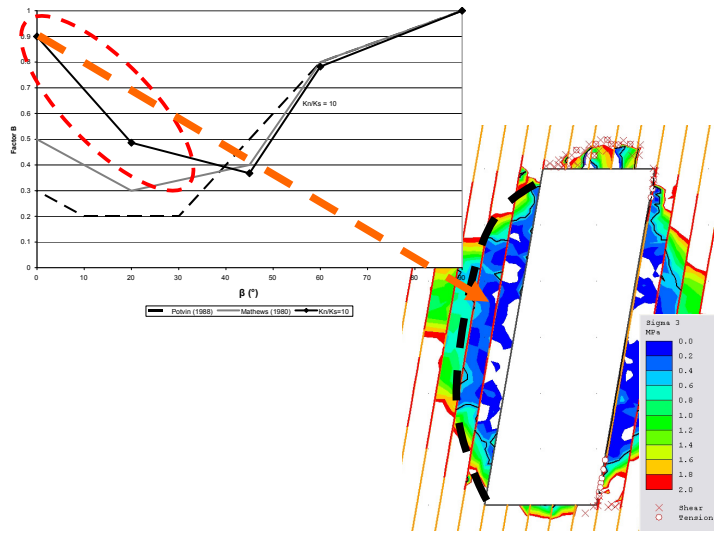


Figure 5: Results for joints parallel ( $\beta = 0^\circ$ ) to the hanging wall of the stope which shows little influence on stress ‘flow’ around the stope and thus restricts the depth of relaxation for this unique simulation. Any flaw that allows failure of “beams” will deepen the  $\sigma_3$  contour and thus drop  $B$ . Joint spacing = 2m,  $K_H/K_S = 10$ ,  $k_o = 1$ , and  $\phi = 40^\circ$ .

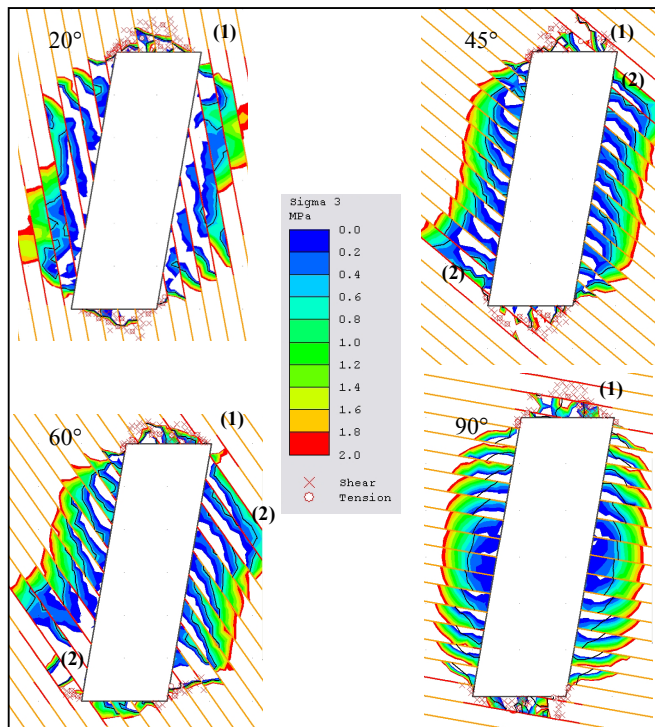


Figure 6: Results for joints oriented  $20^\circ$ ,  $45^\circ$ ,  $60^\circ$ , and  $90^\circ$  to the stope hanging wall which show how the ‘flow’ of stress and thus the level of confinement is changed around the stope boundary depending on joint orientation. Joint spacing = 2m,  $K_H/K_S = 10$ ,  $k_o = 1$ , and  $\phi = 40^\circ$ .

To assess the influence of degrading inter-joint rock mass strength and to determine if this controls the shape of the  $B$ -curve at  $\beta$  angles  $<45^\circ$ , a sensitivity study was completed using four GSI values: 80; 60; 40; and 30 for a 3 m zone surrounding the slope boundary. The results of this analysis are presented on Figure 7 which shows that as GSI is reduced around the slope boundary zone, the Factor B curve between  $\beta$  angles of  $0^\circ$  and  $<45^\circ$  drops rapidly towards the empirically derived curves. A shift to lower Factor B values is also noted between  $\beta$  angles of  $45^\circ$  and  $60^\circ$ . The drop in this area ( $45^\circ$  and  $60^\circ$ ) is less pronounced compared to the shift between  $\beta$  angles of  $0^\circ$  and  $<45^\circ$ .

Taking both the confinement on joints and the strength of the rock mass surrounding the slope boundary into account, the Factor B curves proposed by Mathews et al. and Potvin et al. can be reasonably well reproduced numerically for the slope hanging wall.

The model shows that the Factor B curve for the hanging wall is controlled by two factors:

- (1) the confinement on joints (or faults) ( $\beta$  angles between  $45^\circ$  and  $90^\circ$ ); and
- (2) the inter-joint rock mass strength ( $\beta$  angles between  $0^\circ$  and  $<45^\circ$ ).

Consequently, persistent structure alone are less critical than suggested by the  $B$ -charts between  $\beta$  angles of  $0^\circ$  &  $45^\circ$ , but when combined with a rock mass that can disintegrate ( $>3$  joint sets), the available charts are representative. This is consistent with the fact that rock masses in the databases involve moderately jointed rock masses.

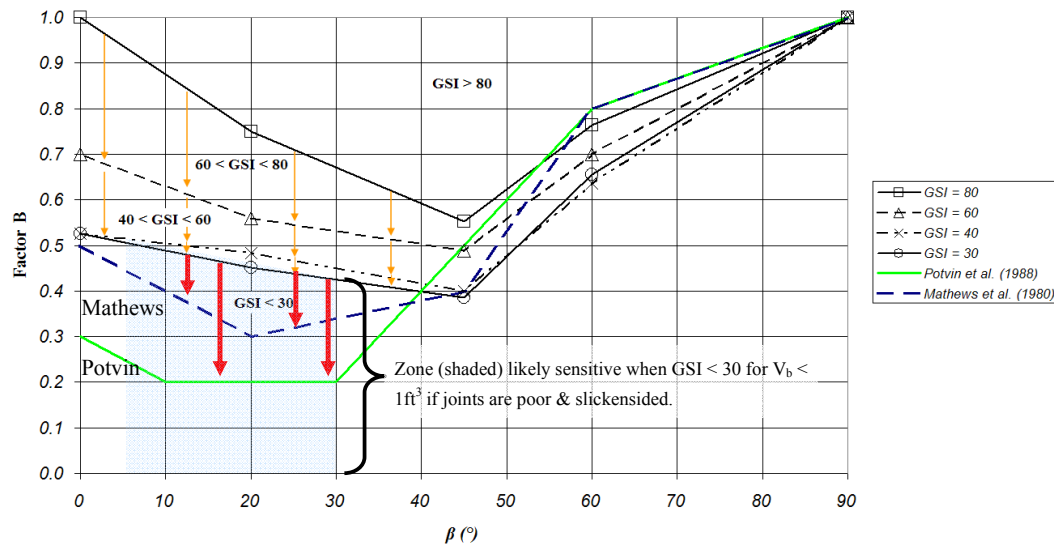


Figure 7: Influence of GSI on the shape of the Factor B curve. Joint spacing = 2m,  $K_n/K_s = 10$ ,  $k_o = 1$ , and  $\phi = 40^\circ$ .

### 3.2 Slope Back

A typical set of numerically derived Factor B results for the slope back are presented on Figure 8. The results are again compared to both the Factor B curves proposed by Mathews et al. (1980) and Potvin et al. (1988). The numerical modelling derived Factor B curves for the slope back are not similar to the empirically derived. The curves do have the same general shape but do not have the same magnitude as compared to the empirical curves. These results could be because Mathews et al. (1980) and Potvin et al. (1988) did not consider a separate Factor B curve for the slope back but more likely because of the modelled ratio of joint spacing to excavation span has a predominant influence (i.e. scale effect).

The slope back has a smaller span (10 m) compared to the slope hanging wall (30 m). With a smaller span, the slope back is not as frequently intersected by joints and will in general behave as a more stable excavation face (as long as the rock mass strength between the modelled structures is high). Smaller spacing values were attempted to be modelled but were not successful

due to impractical modelling computation times. To assess the potential scale effect, the span of the slope back was increased to 20 m. The model results for the larger slope back span push the Factor B curve down closer to the empirically derived curve between  $0^\circ$  and  $90^\circ$  (Figure 8).

The influence of rock mass strength on slope back stability was not modelled but it is reasonable to assume based on the results for the slope hanging wall (Figure 7) that for  $\beta$  angles between  $0^\circ$  and  $<45^\circ$ , the curve would tend towards the empirically derived curves.

Based on the observed large difference between the numerically derived Factor B curves for the slope hanging wall and back, separate curves may need to be developed for these respective slope faces due to potential scale effects. An assessment of the available empirical slope stability data was assessed by Bewick (2008) but is not discussed here.

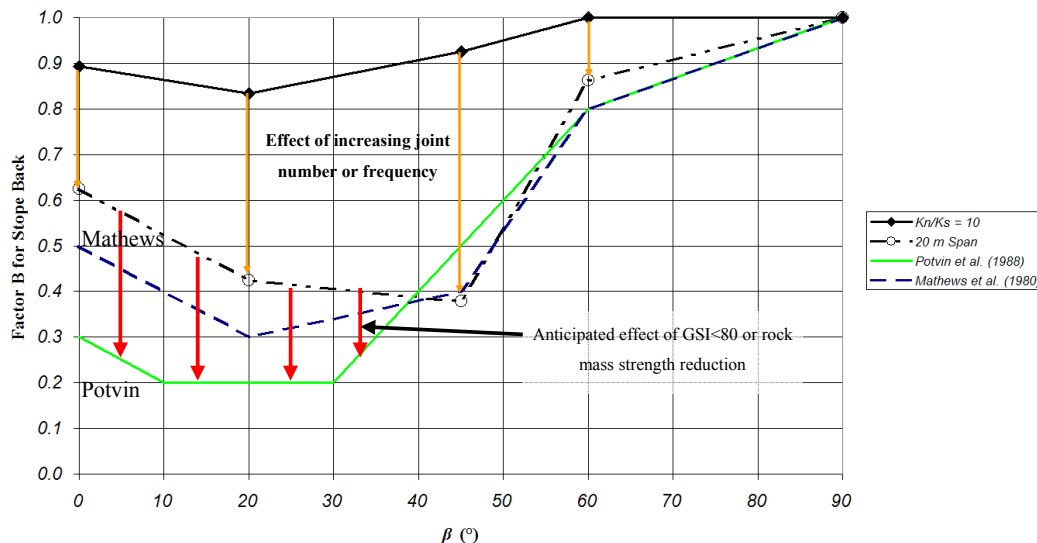


Figure 8: Typically numerically derived Factor B curve for the slope back. Joint spacing 2m,  $K_n/K_s = 10$ ,  $k_o = 1$ , and  $\phi = 40^\circ$ . Arrows show effect of joint spacing due to slope back span increasing from 10m to 20m (from 5 to 10 structures intercepting slope back).

#### 4 PARAMETRIC ANALYSIS

Joint spacing, stiffness ratio ( $K_n/K_s = 1, 10, \& 20$ ), joint friction ( $\phi = 30^\circ, 40^\circ, \& 50^\circ$ ), in situ stress ratio ( $k_o = 0.5, 1.0, 1.35, 1.5, \& 2.0$ ), and GSI (values of 80, 60, & 40) were varied. Based on the sensitivity study, the selected joint stiffness ratios of 1, 10, and 20 did not show a significant change in the shape of the Factor B curve. The influence of GSI around the slope boundary for the hanging wall has been discussed in Section 3.1 and is a predominant factor. Therefore, only the influence of joint friction, joint spacing and in situ stress ratio will be discussed here. Full results can be found in Bewick (2008).

##### 4.1 Joint Friction

The results for the influence of joint friction ( $\phi$ ) on the shape of the Factor B curve are presented on Figure 9 for the slope hanging wall. Joint friction has a large influence on the shape of the hanging wall Factor B curve. These observations are contrary to Potvin et al. (1988) where they assumed that the influence of joint friction was sufficiently taken into account through the ratio of  $J_r/J_a$  in the  $Q'$  component of  $N'$ . As joint friction increases, the influence of joint orientation is reduced and the curve becomes 'flatter' (as long as the rock mass strength is high). In addition, the influence of joint orientation between  $0^\circ$  and  $20^\circ$  is reduced for higher joint friction values (i.e. approximately 0.7 for  $\phi = 40^\circ$  and  $50^\circ$  compared to approximately 0.5 for  $\phi = 30^\circ$ ). The lower friction value  $\phi = 30^\circ$  results in a more 'trough' shaped curve. It is expected that higher friction values  $>50^\circ$  will keep flattening the Factor B curve while lower

friction values  $<30^\circ$  will deepen the trough of the curve and continue to shift the curve towards the smaller numbers on the chart.

Based on the numerical results for the hanging wall in high strength rock masses:

- When  $\phi > 40^\circ$ , there is less influence of joint orientation for  $\beta$  angles  $>20^\circ$  and  $45^\circ$  because of the increased shear resistance due to the high joint friction angle minimizing shear yield along the joint elements and maintaining confinement closer to the boundary of the stope;
- When  $\phi < 40^\circ$ , there is more influence of joint orientation for  $\beta$  angles  $>20^\circ$  and  $90^\circ$  (i.e. stability is affected even at high joint angles) because of the lower shear resistance due to lower joint friction allowing joint element shear, pushing lower confinement conditions further away from the stope boundary; and
- When joints are oriented at  $\beta$  angles  $<20^\circ$ , there is no to little influence of joint friction on the shape of the Factor B curve and thus stability because at the lower  $\beta$  angles, instability is dominated by the strength of the inter-joint rock mass strength (ref. – 3.1 and Figure 7) oppose to the orientation of the dominant structures around the stope boundary.

A query of the case history data published by Potvin et al. (1998) was assessed to determine if any data was available to confirm the numerical friction based results. As no specific joint property data is listed in the case history databases, no direct back correlation could be completed to confirm the joint friction dependent Factor B curves (Bewick, 2008). Potvin et al. (1988) do list the ratio of  $J_r/J_a$  but the structure of the database is not amenable to properly look at the influence of joint friction. More work is needed looking at  $J_r$  and  $J_a$  values in the calibration database of Potvin et al. (1988).

It should be noted that Figures 9 to 11 are for “strong” rock masses. Lower, B-curves would be expected for  $GSI < 70$ .

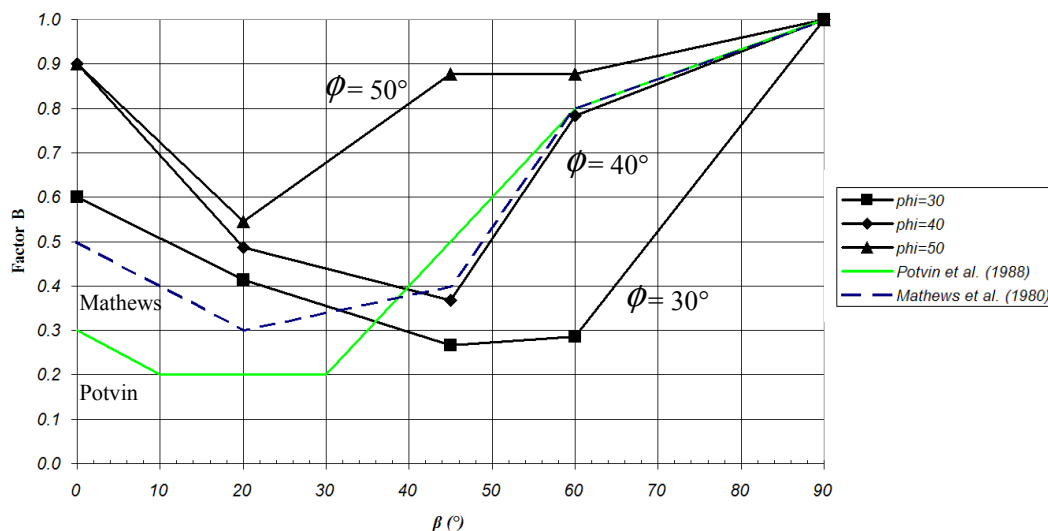


Figure 9: Effect of joint friction ( $\phi$ ) on stope hanging wall stability ( $k_o = 1$ , joint spacing of 2 m, and  $K_{tr}/K_s = 10$ ).

#### 4.2 Joint Spacing

The results for the influence of joint spacing on the shape of the Factor B curve are presented on Figures 10 & 11 for the stope hanging wall and back respectively.

For a stope hanging wall in high strength rock (Figure 10), as joint spacing reduces from 8 m to 2 m the Factor B curve shifts slightly lower. But in general, no significant change occurs in the shape of the Factor B curve.

For the stope back in high strength rock (Figure 11), little to no change occurs in the Factor B curves unless a stope back span of 20 m is modelled (i.e. the joint frequency is high). This is

twice that of the base model of 10 m which effectively models the case of 1 m spaced joints considering excavation span to joint spacing ratio. Based on the excavation span to joint spacing ratio (scale effect), when the stope back span is increased to 20 m the influence of joint spacing becomes evident. There also appears to be less influence of joint orientation on stope back stability for excavation span to joint spacing ratios  $\leq 10$  based on the current modelling results. This observation is opposite to that observed when looking at the results for the hanging wall where no scale effect was evident based on the modelled joint spacing values. This is likely a result of the stope geometry and large hanging wall span.

In general, closer joint spacing values result in less stable stope walls. Although, even when joints are spaced up to 8 m apart, joint orientation still influences hanging wall stope stability roughly on the same order of magnitude as the 4 m and 2 m joint spacing values. Joints spaced at these large spacing values still influence the stress field around the hanging wall and low confinement is still propagated deeper into the hanging wall rock mass.

While smaller joint spacing values of  $< 2$  m were not modelled, it is expected that the curve would continue to shift down and influence stope wall and back stability to a greater extent.

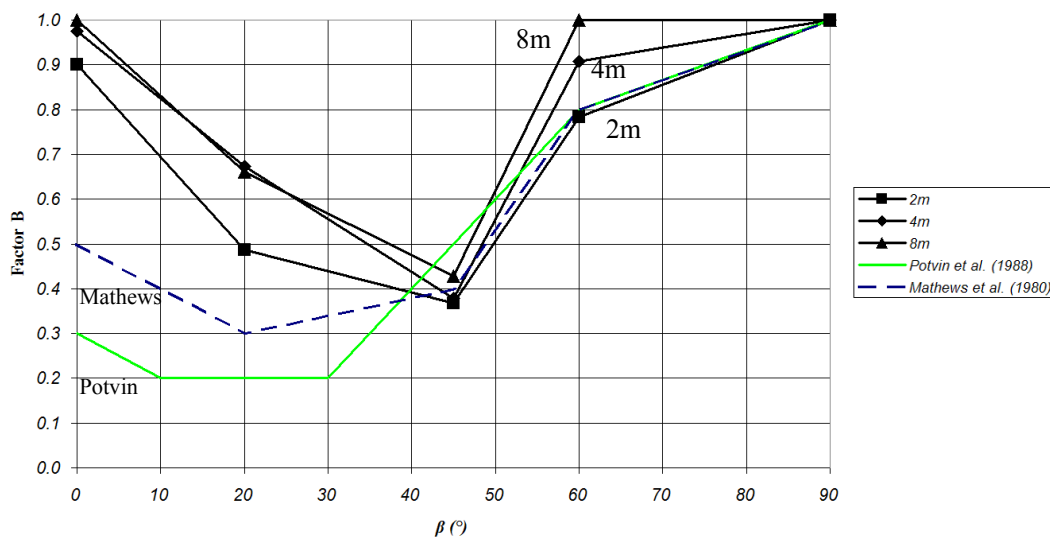


Figure 10: Effect of joint spacing on stope hanging wall stability ( $k_o = 1$ ,  $\phi = 40^\circ$ , and  $K_n/K_s = 10$ ).

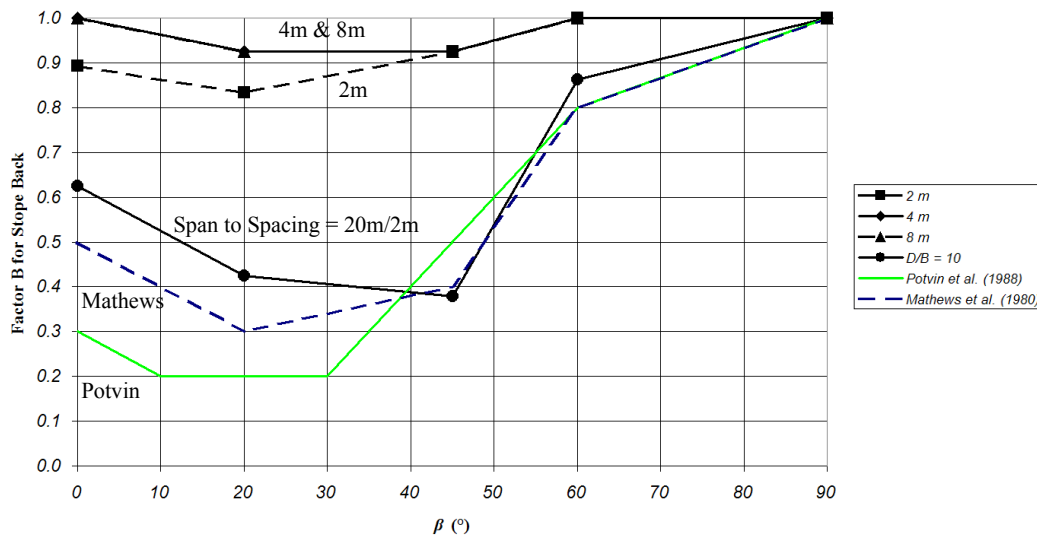


Figure 11: Effect of joint spacing on stope back stability ( $k_o = 1$ ,  $\phi = 40^\circ$ , and  $K_n/K_s = 10$ ). D/B is the span to spacing ratio ( $20\text{m}/2\text{m} = 10$  for the larger stope back span).

### 4.3 In Situ Stress Ratio ( $k_o$ )

While the in situ stress ratio is of importance for initial design considerations, once mining initiates and progresses, excavations can experience a number of stress states over time. The effect of different stress ratios on the Factor B curve could allow for the influence of mining induced stress change to be considered outside of the stress Factor  $A$  which accounts for the influence of stress on slope stability. The main benefit of considering the influence of stress in addition to joint orientation is that the Factor  $A$  (rock stress factor) only assesses the possibility of rock mass failure and not failure in combination with a major persistent critical joint set or structure.

The results for the influence of in situ stress ratio ( $k_o$ ) on the shape of the Factor B curve are presented on Figure 12 for the stope hanging wall. The results for the stope back are not presented but discussed.

For the hanging wall (Figure 12), as the stress ratio increases from 0.5 to 2.0, the curves between  $\beta$  angles of  $45^\circ$  and  $90^\circ$  shift to lower Factor B values while the  $k_o = 1.5$  falls outside of the observed trends. Based on the results for the hanging wall in a high strength rock mass (not considering the potential  $k_o = 1.5$  outlier):

- As the stress ratio increases from 0.5 to 2.0, there is more influence of joint orientation between  $\beta$  angles of  $>45^\circ$  and  $90^\circ$ ; and
- As the stress ratio increases from 0.5 to 2.0 there appears to be generally less influence of joint orientation between  $\beta$  angles of  $0^\circ$  and  $45^\circ$ .

The influence of  $k_o$  on the stope back was not as evident. Similar to the HW, as the stress ratio increases from 0.5 to 2.0, the curves between  $\beta$  angles of  $45^\circ$  and  $90^\circ$  generally shifted to lower Factor B values.

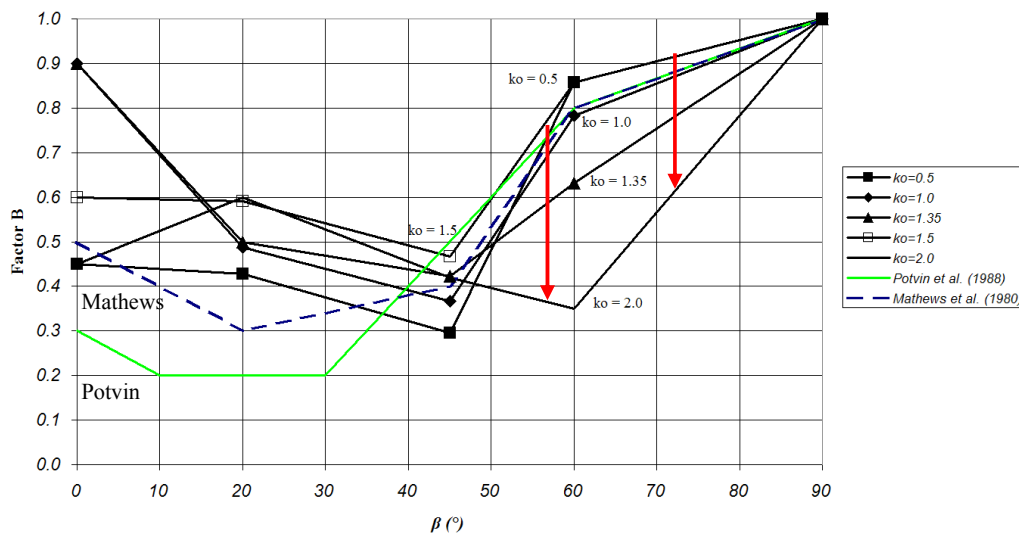


Figure 12: Effect of stress ratio ( $k_o$ ) on stope hanging wall stability ( $\phi = 40^\circ$ , joint spacing of 2m, and  $K_n/K_s = 10$ ).

## 5 CONCLUSIONS

The shape of the empirical Factor B curve proposed by Mathews et al. (1980) and Potvin et al. (1988) could be reasonably reproduced using a 2D continuum numerical modelling approach that included joint elements considering confinement and joint orientation alone for the stope hanging wall between  $\beta$  angles of  $45^\circ$  and  $90^\circ$ . Between  $\beta$  angles of  $0^\circ$  and  $<45^\circ$ , the strength of the rock mass between the joint elements had to be considered around the near boundary of the stope because joint orientation was no longer dominating the lowering of confinement around the stope boundary. This clearly shows that persistent structure alone (within a strong rock

mass) are less detrimental to slope stability, but if combined with a fragile rock mass that can yield or spall can be very detrimental.

The mechanisms affecting the Factor B curve appear to be grouped into two zones:

- Joint Confinement ( $\sigma_3$ ):  $\beta$  angles  $45^\circ$  and  $90^\circ$ ; and
- Inter-Joint Rock Mass Strength:  $\beta$  angles  $0^\circ$  and  $<45^\circ$ .

This suggests that if the rock blocks surrounding the slope boundary are very strong, the Factor B curves proposed by Mathews et al. (1980) and Potvin et al. (1988) are too conservative at lower  $\beta$  angles ( $0^\circ$  and  $<45^\circ$ ) because the zone of low confinement is maintained relatively close around the slope boundary. If the rock blocks surrounding the slope boundary are weak or friable (i.e. ready to fracture), the influence of persistent joint/fault structures is less dominant between  $\beta$  angles  $0^\circ$  and  $<45^\circ$  and controlled by the inter-joint rock mass strength.

Joint friction ( $\phi$ ) and stress ratio ( $k_o$ ) were determined to have the most influence on the shape of the Factor B curve. It cannot be assumed that joint friction is fully accounted for in the  $Q'$  value within the stability number  $N'$ .

## 6 ACKNOWLEDGEMENTS

The main Author would like to thank: staff at MIRARCO namely Fidelis Suorineni, Bo-Hyun Kim, and Ming Cai for their insightful discussions; the mining group staff at Golder Associates Ltd. Sudbury namely Kevin Beauchamp & Paul Palmer for allowing me to take the time to complete a master's degree; and my advisor Peter Kaiser for his time and patience. NSERC also deserves mention for the financial support provided through Dr. Kaiser and Trevor Carter for feedback regarding this paper.

## REFERENCES

- Alcott, Jane M., Kaiser, P.K. Gauthier, M. Nelson, D. and Mah, P. 1999. SHARK: stability hazard and risk assesment at Placer Dome's Campbell mine. In Colloque de Contrôle de Terrain, Val-d'Or, QU:9 p.
- Barton, N. R., Lien, R. & Lunde, J. 1974. Engineering classification of rock masses for the design of tunnel support. *Rock Mech.*, 6(4): 189-239.
- Bewick, R. P. 2008. Effects of anisotropic rock mass characteristics on excavation stability. MASC thesis, Laurentian University.
- Cai, M., Kaiser, P. K., & Martin, C.D. 1999. Comparative study of rock support system design practice for large-scale underground excavations. GRC, Laurentian University, unpublished report.
- Clark, L.M., and Pakalnis, R.C. 1998. An empirical design approach for estimating unplanned dilution of rock mass relaxation and degradation into empirical slope design. CIM-AGM, Vancouver, 1997, 15pp.
- Corkum, B. 2007. Personnel communication.
- Mathews, K. E., Hoek, E., Wyllie, D. C. and Stewart, S. B. V. 1980. Prediction of stable excavation spans for mining at depths below 1,000 metres in hard rock. Golder Associates report to CANMET. Department of Energy and Resources: Ottawa.
- Potvin, Y., Hudyma, M.R., & Miller, H.D.S. 1988. Volume I – Slope Design. NSERC Project #CRD-8612 Integrated Mine Design.
- Potvin, Y. 1988. Empirical open slope design in Canada. PhD. Thesis, Dept. Mining and Mineral Processing, University of British Columbia.
- RocScience. 2006. Phase<sup>2</sup> Software.
- Suorineni, F. T. 1999a. Effects of faults and stress on open slope design. PhD. Thesis: Univ. of Waterloo.
- Suorineni, F.T., Tannant, D.D., and Kaiser, P.K. 1999b. Determination of fault related sloughage in open slopes. *Int. J. Rock Mech. Min. Sci.*, 36, 891-906.
- Suorineni, F.T., Kaiser, P.K., and Tannant, D.D. 2000. Unifying application of the stability graph for open slope design. Paper submitted to CIM Bull.
- Zhang, Y. and Mitri, H. S. 2007. Stability assessment of non-entry stopes using nonlinear finite element analysis. *Rock Mechanics: Meeting Society's Challenges and Demands – Eberhardt, Stead & Morrison (eds).* Taylor & Francis Group, London.